Comparison of standard geophones and newly designed horizontal detectors

GEOPHYSICS, VOL. 66, NO. 6 (NOVEMBER-DECEMBER 2001); P. 1827–1837, 15 FIGS., 3 TABLES.

Comparison of standard horizontal geophones and newly designed horizontal detectors

L. Sambuelli*, G. P. Deidda‡, G. Albis**, E. Giorcelli§, and G. Tristano**

ABSTRACT

To increase the speed and efficiency of shallow seismic *SH*-wave data recording and to decrease acquisition costs, we have designed, constructed, and tested a new velocity tool that detects horizontal movements better than standard horizontal geophones. A comparative evaluation of significant characteristics and field performances of this new detector was conducted through laboratory and field tests on two sets of receivers: one consisting of 24 prototypes of the new detector and the other consisting of 24 standard horizontal geophones. Laboratory measurements revealed similar behaviors of impedance curves and geophone responses for the two types of detectors, but the impedance amplitudes and the frequency-response amplitudes of the new detector were twice those of the standard geophones. However, comparison of the horizontal-to-vertical (response) ratios, proved that the new detector better discriminates (6 dB on average) between the horizontal and vertical excitements. Field data proved that the energy, the maximum amplitude in the trace, and the maximum reflected amplitude were always higher in the data recorded with the new detector, although only half the source energy was used. The extra cost and weight of the new detector should be outweighed by its advantages, such as higher sensitivity to horizontal motions, better energy efficiency, and greater cost effectiveness. When a wavefield can be interpreted as *SH*-waves, *SH*-wave records can be acquired without the traditional drawbacks such as acquiring two records in each shot position, preprocessing of each record, and the final trace-to-trace subtraction needed to produce a pure *SH*-wave record.

INTRODUCTION

During the last 20 years, the seismic reflection method—the mainstay of oil and gas exploration—has been increasingly applied as a tool for imaging shallow targets in engineering, mining, groundwater, and environmental investigations (e.g., Ziolkowski and Lerwill, 1979; Doornenbal and Helbig, 1983; Hunter et al., 1984; Singh, 1986; Birkelo et al., 1987; Jongerius and Helbig, 1988; Miller et al., 1989; Steeples and Miller, 1990; Miller and Steeples, 1990, 1991).

Several authors (e.g., Stumpel et al., 1984; Milkereit et al., 1986; Hasbrouck, 1991; Goforth and Hayward, 1992; Dobecki, 1993; Clark et al., 1994; Jeng, 1995) have demonstrated that certain geophysical objectives could be addressed more effectively using *SH*-waves rather than *P*-waves; nevertheless, *SH*-waves are not widely used since they involve higher costs than *P*-waves. When suitable circumstances occur and the appropriateness of the method is verified, the key to the successful use of shallow seismic reflection is its cost effectiveness, that is, low-cost data acquisition and minimal data processing (Steeples et al., 1997).

Traditionally, *SH*-wave data acquisition uses polarized sources. *SH*-wave records require two shots, striking the source in opposite directions perpendicular to the seismic line, which must be subtracted to eliminate *P*-wave contamination (Helbig, 1987; Hasbrouck, 1991). This means an increase in survey costs compared to similar *P*-wave surveys. It is also common that effective *P*-wave removal requires adjusting amplitude (rescaling) and removing time-break variations (determined by crosscorrelation) of shot records before subtraction (McCormack and Tatham, 1986). This means additional processing time and, as a consequence, additional costs.

We present a new geophone apparatus (Sambuelli and Deidda, 1998, 1999) composed of two standard horizontal

Manuscript received by the Editor October 25, 1999; revised manuscript received March 2, 2001.
*Politecnico di Torino, Dipartimento di Georisorse e Territorio, Corso Duca Degli Abruzzi, 24, Torino, Italy. E-mail: sambuelli@polito.it.
‡University di Cagliari, Dipartimento di Ingegneria del Territorio, Sezione di Geologia Applicata e Geofisica Applicata, Piazza d'Armi, 16,09123 Cagliari, Italy. E-mail: gpdeidda@unica.it.
**Politecnico di Torino, Dipartimento di Elettronica, Corso Duca Degli Abruzzi, 24, Torino, Italy. E-mail: albis@polito.it.
§Politecnico di Torino, Dipartimento di Meccanica, Corso Duca Degli Abruzzi, 24, Torino, Italy. E-mail: giorcelli@polito.it.

geophones connected to detect horizontal movements better than standard geophones. When the horizontal components of the wavefield can be interpreted as SH-waves, the newly designed detector enables acquisition of SH-wave data without additional costs. Using this detector, SH-wave records with minimal P-wave contamination can be acquired performing single shots and avoiding extra processing. Consequently, SH-wave surveys can be performed in the same way as P-wave surveys without involving traditional extra costs.

To show the performance of the new horizontal velocity detector, we tested 24 prototypes both in the laboratory and field, and compared the results to 24 commercial horizontal geophones. We only considered 100-Hz receivers, which are widely used in shallow seismic reflection. All the test results proved the superiority of the new detectors over traditional ones. The evident drawbacks, such as higher costs and weight, may well be outweighed by their better technical characteristics and the inexpensiveness of their use, so they can be considered an improvement in SH-wave reflection seismology that could be of great assistance to engineering seismologists.

METHODS

To quantify the significant characteristics and field performances of the new detector, laboratory and field tests were conducted with consistent testing procedures and equipment. All the tests were conducted on two sets of receivers to make an effective comparison; one of them was made up of 24 new horizontal detectors, and the other consisted of 24 Mark Products (L-40 A2) 100-Hz horizontal geophones. The specifications obtained from the manufacturer for the L-40 A2 geophones are listed in Table 1.

Brief description of the new horizontal velocity detector

The horizontal velocity detector prototype has two horizontal 100-Hz geophones combined with special mechanical and electrical arrangements. The geophones are mounted onto a common support so their axes are inclined in opposite directions at an angle 87° from the vertical (Figure 1). When the detector is positioned for use, both geophone axes lie on the vertical plane perpendicular to the receiver-line orientation. As for the electrical arrangement, the two elements are connected in push–pull series to yield a seismic trace in which the horizontal component is accentuated while the unwanted vertical component is attenuated.

Although the detector does not have to be leveled as carefully, in that any slight misleveling will change the amount of vertical motion already expected because of the nonhorizontal alignment of their elements, it has a leveling bubble molded into the top of the casing to ensure a horizontal setting within ±3° of tolerance. Coupling to the ground is ensured through an 8-cm spike; however, it is very important to plant the receiver with its base firmly touching the ground (this is true for all horizontal geophones).

Table 1. Mark Geophone (L-40 A2) specifications.

Characteristic	Specification
Frequency (f_0)	100 Hz ± 7%
Coil resistance (R_c)	510 Ω ± 10%
Transduction constant (G)	0.2755 V/cm/s
Open circuit damping (b_0)	0.479

Laboratory tests

Electrical and mechanical tests were carried out. The electrical measurements were made with an HP 4192A impedance analyzer. The impedance of the device under test (DUT) was determined by the vectorial ratio between the applied voltage and the current flowing through the DUT. The maximum uncertainty on the impedance modulus is a function of frequency and has been estimated to be lower than 0.1%. Three hundred amplitude and phase values were collected in a frequency range spanning from 10 Hz to 10 kHz (100 values/decade); the amplitude of the input voltage was equal to 0.2 V rms for all the tests.

The test apparatus (Figure 2) was used to determine geophone response. The tested receivers were bolted onto a shaker (Unholtz Dickie), which was vibrated with harmonic motion of constant maximum amplitude (1 cm/s) using a 10–1250-Hz sweep in frequency. The sweep rate was 1 oct/min. The reference chain consisted of a Brüel & Kjær model 4383 accelerometer and a Brüel & Kjær model 2635 charge amplifier with single temporal integration to obtain a speed measurement. The accelerometer was placed on the shaker 5 cm from the tested geophone. The sensitivity of the reference chain of measure was equal to 100 mV/cm/s. The output signals from the geophones and the reference chain were acquired with a Data Physics board, and the frequency response function $H(f)$ was calculated by

$$H(f) = \frac{U_{geophone}(f)}{V_{ref}(f)}\left[\frac{\mathrm{V}}{\mathrm{m/s}}\right], \qquad (1)$$

where $U_{geophone}(f)$ is the output signal from the geophones, $V_{ref}(f)$ is the oscillation velocity measured by the reference chain, and f is the frequency. The test frequency range was

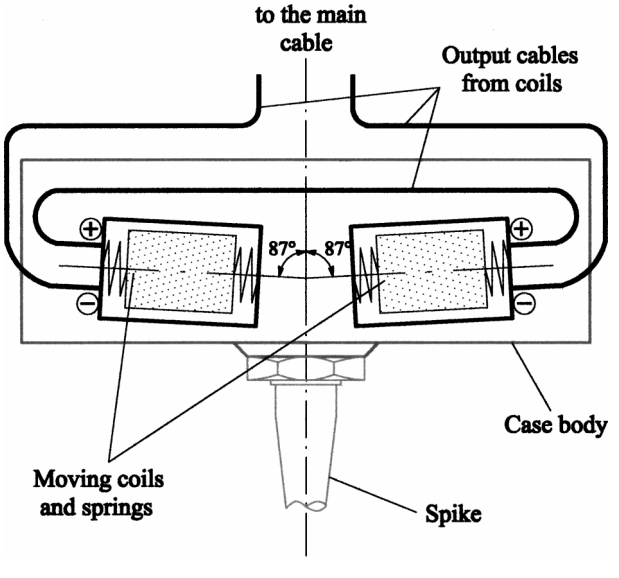

FIG. 1. Schematic of the new horizontal velocity detector. The two basic units are connected in series but with the polarities of one of them reversed.

0–1250 Hz with 1000 spectral lines, so the spectral resolution was 1.25 Hz. In this way, it was possible to calibrate the signal coming from the geophones for each kind of test, obtaining geophone sensitivity curves. All the horizontal receivers were excited in both the vertical and horizontal directions.

Field test

The field test was carried out, under ideal conditions (windless day, noiseless environment), on a real-scale ground model built in a quiet flatland far from any artificial source of vibrations. The reflecting horizon at the test site is the top of a concrete layer located 3.5 m below the ground surface overlain by alluvial material.

An ABEM Mark VI seismograph recorded the data digitally in SEG-2 format. Instrument specifications and recording parameters used in the field test are listed in Table 2. Receiver offsets ranged from 0.6 to 5.2 m, with a group interval of 0.2 m. Two different horizontal velocity detectors were firmly planted and alternatively connected to the seismic cable for each of the 24 receiver stations.

The seismic source was selected to meet repeatability requirements. For this purpose, we used a 10-kg sledgehammer, swung through an arc, that struck a 70-kg steel plate (Figure 3). The latter, anchored to the earth by stakes driven into the ground, was loaded with 100 kg of lead after being seated with several hammer impacts. The striking mass was allowed to fall freely from a height of 2.05 m to a height of 0.05 m. The sledgehammer struck the plate with a single blow for each record. In this way, we were able to limit the modification of the soil characteristics below the baseplate, thus improving repeatability. No problem resulted from our having used low energy, since the absence of ambient noise and the low depth of the high-impedance contrast reflector allowed good S/N ratio. Regarding the trigger circuit, one pole of the cable was connected to the falling metal mass while the other was connected to the metal plate. In this way, the closing of the circuit determines the start of recording. Possible time-break variations were therefore the result of the internal trigger circuit.

The data were recorded with no low-cut filtering, 100-Hz low-cut filtering, and 240-Hz low-cut filtering for both receiver sets. When standard horizontal geophones were used, two records were collected for each filtering set-up striking the source in opposite directions perpendicular to the receiver profile (Figure 3). When using the new detectors, only one record was collected striking the source at the right end.

ANALYSIS AND RESULTS

Figure 4 shows the complex impedance as a function of frequency. The curves show similar behavior. The only significant difference noticed in the graphs is that the amplitude of the new detector impedance (Figure 4b) is double that of the standard geophone (Figure 4a). This is obvious since in the new detector there are two elements connected in series. No differences are present in the phase impedance curves. Coil resistance and open circuit damping, which were also measured in the tests, are listed in Table 3. The measured values are in good agreement with those listed on the manufacturer's sheet (Table 1).

Typical data obtained in mechanical tests are shown in Figures 5 and 7. Figure 5 shows the measured geophone responses for the standard (Figure 5a) and new (Figure 5b) detectors. The amplitude responses show the same behavior and can be matched by decreasing the new detector response by a factor of two; the phase responses, instead, are quite identical. For both receivers, above the natural frequency and up to about 600 Hz, the phase is nearly linear and the amplitude is flat, with a response determined by the sensitivity of the receivers. In fact, as shown in Figure 6, by superimposing the theoretical responses obtainable from equation

Table 2. Seismograph specifications and recording parameters.

Characteristic	Parameter
Number of channel	24
A/D converter	18 bits
IFP amplifier	3 bits
Dynamic range	114 dB
Instrument noise	120 nV (rms)
Slope of the (used) analog low-cut filters	24 dB/oct
Record length	400 ms
Sample interval	0.1 ms

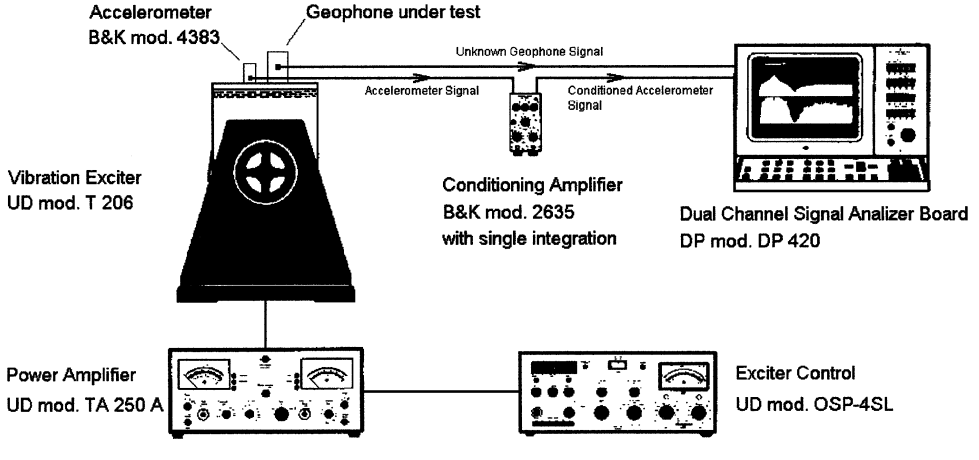

FIG. 2. Schematic of the apparatus for mechanical tests.

$$M = \frac{G}{\sqrt{\left[1 - 2(1 - 2b_0^2)\left(\frac{f_0}{f}\right)^2 + \left(\frac{f_0}{f}\right)^4\right]}}, \qquad (2)$$

when f_0 (natural frequency) and b_0 (open circuit damping) equal the values in Table 3, the measured and calculated responses can be matched if the transduction constant (G) is 0.2740 V/cm/s for standard and 0.5506 V/cm/s for the new detector. At about 600 Hz, the measured amplitudes start to increase up to a peak of about seven times the flat-frequency value. The peak in the amplitude at 1000 Hz is almost certainly from the receiver shaker coupling. The resonance coupling is probably caused by the tendency of the receivers to rock instead of move horizontally with the shaker. In the field, this rocking was attenuated by placing the base of the receivers firmly on the ground.

The responses for the receivers excited in the vertical direction (with the receiver axis perpendicular to the shaker axis) are plotted in Figure 7. These curves present some departures from clean responses which alter the general aspect and make interpretation difficult. For present purposes the comparison between the horizontal-to-vertical (response) ratios for the two types of receivers seems to be more significant (Figure 8). For all frequencies the ratio is better (higher) for the new detector. That is, it has an increased response to the horizontal motion (on average 6 dB) and better discriminates between the horizontal and vertical excitements.

To compare the performance of the two types of receivers, the field test results are presented as

1) variable-area wiggle-trace plots to allow the reader to make trace-to-trace and file-to-file comparisons of wavelet characteristics and relative energy of different phase mode waves;
2) energy (measured as the trace variance) and true amplitude plots to show trace by trace the differences in energy content, amplitude maxima measured on the whole record time window, and amplitude maxima measured on a time window including only reflected signal; and
3) amplitude spectra plots to compare the spectral characteristics of signals recorded with the two types of receivers considered in the test.

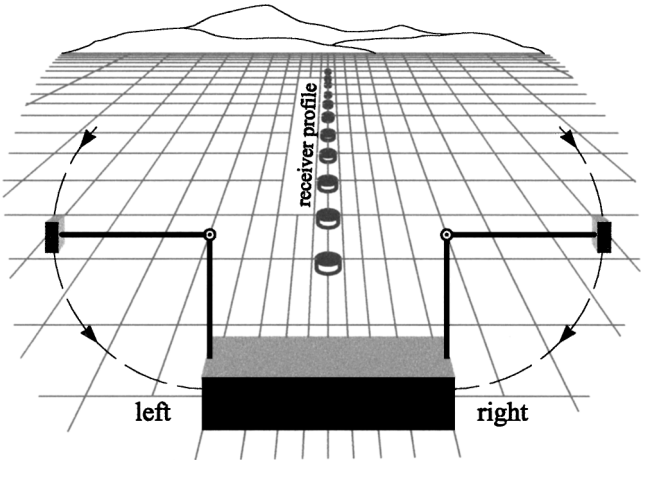

FIG. 3. Schematic of the polarized source used to generate SH-waves. Using standard horizontal geophones, the baseplate was struck first on the right side and then on the left; while using new horizontal detectors, the baseplate was struck only on the right side.

The first arrival on all the seismograms is the airwave. However, on the unfiltered records, the amplitude of the airwave is very small in comparison to later arrivals, and its presence is

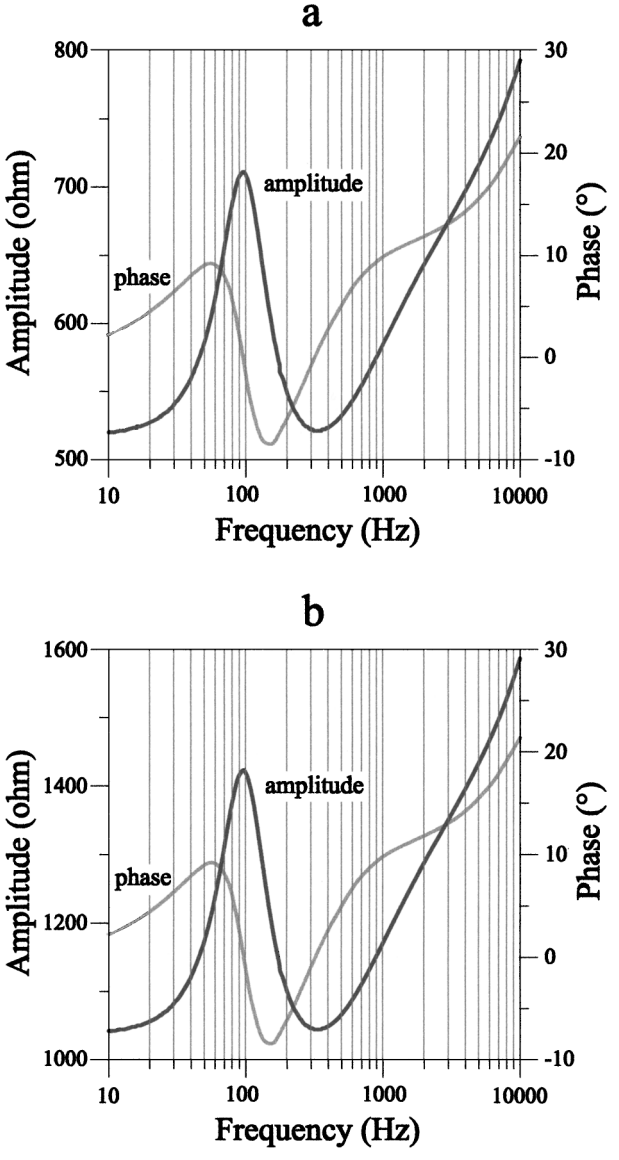

FIG. 4. Complex impedance (amplitude and phase) curves as from the electrical tests conducted on (a) a standard horizontal geophone and (b) on the newly designed horizontal detector.

Table 3. Measured characteristics for the two set of detectors.

Characteristic	Mark geophone	New detector
Frequency (f_0)	98.56 Hz	95.63 Hz
Coil resistance (R_c)	504.11 ± 11.37Ω	1008.23 ± 11.70Ω
Transduction constant (G)	0.2740 V/cm/s	0.5506 V/cm/s
Open circuit damping (b_0)	0.486	0.499

not always apparent. The first post-airwave coherent event on the records is the direct *P*-wave, which has a velocity measured at 130 m/s. On all records, the prominent events are the direct *SH*-wave and the reflected *SH*-wave. The latter event is the wide-angle reflection from the overburden/concrete interface 3.5 m below the ground surface, which is characterized by a velocity of 72 m/s.

All field records are displayed in relative-amplitude, wiggle-trace, variable-area format without gain. As usual, the seismograms relative to standard horizontal geophones are

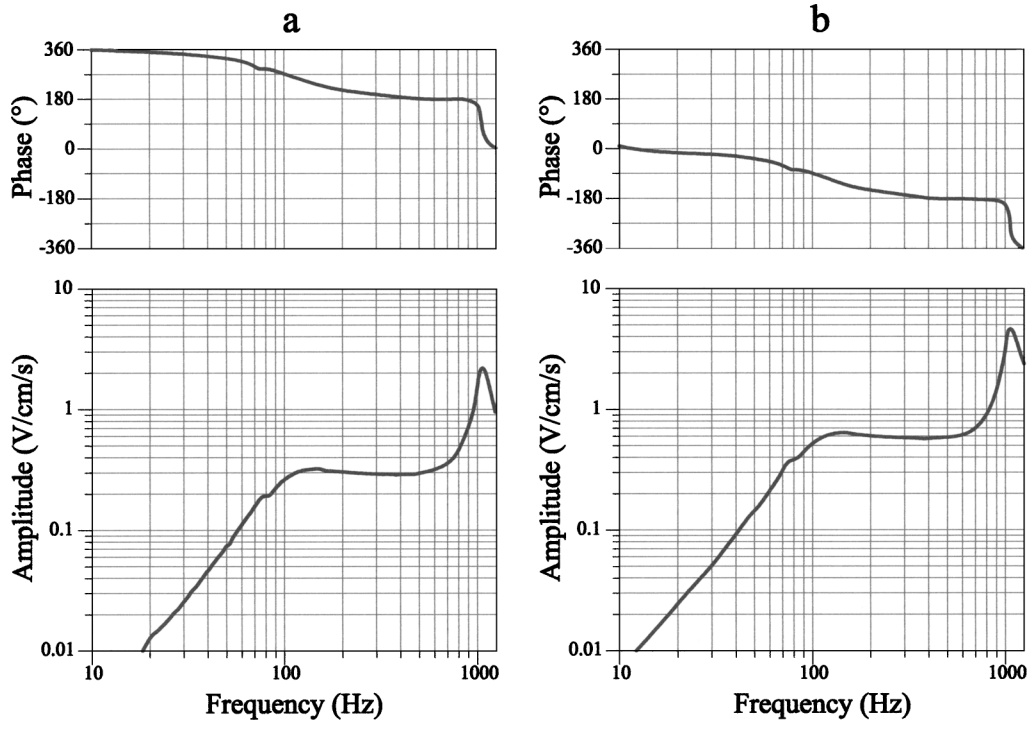

FIG. 5. Geophone responses for (a) a standard horizontal geophone and (b) the new detector set up horizontally and excited in the horizontal direction.

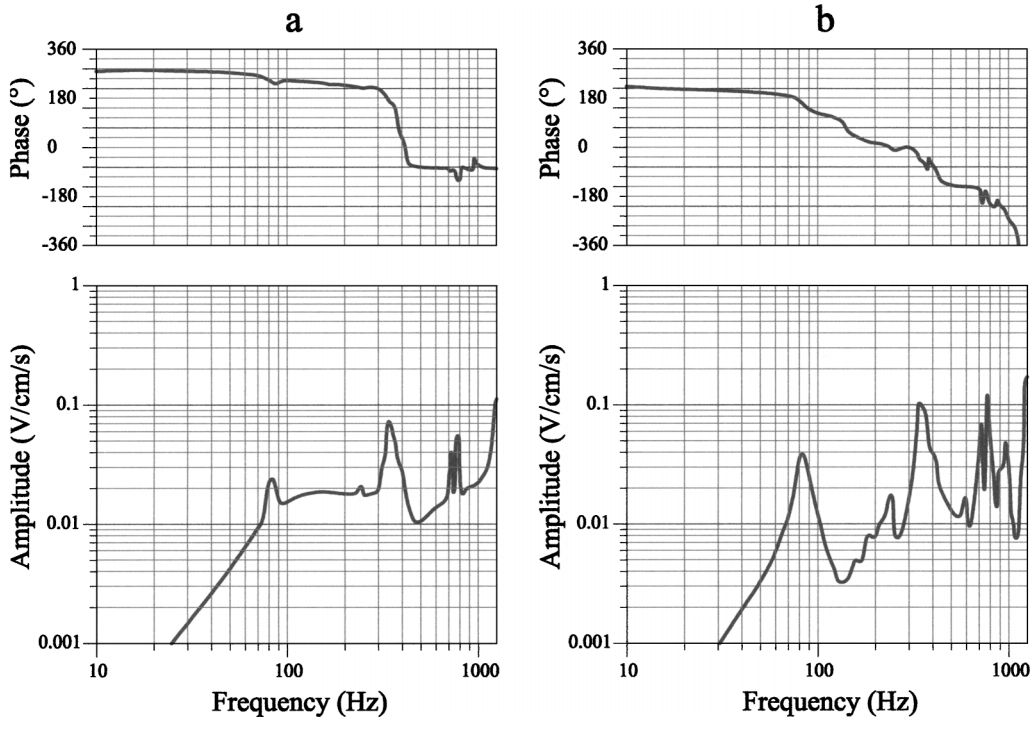

FIG. 6. Geophone responses for (a) a standard horizontal geophone and (b) the new detector set up horizontally and excited in the vertical direction.

obtained by summing two field records (right and left) after having reversed the polarity of one of them (Figure 9). Before summing, time-break variations were carefully checked and then removed by cross-correlation techniques, and amplitude-rescaling processing was executed. No other processing steps alter these records. The data recorded using new detectors were not subjected to any kind of processing. Figures 10–12 compare the records, corresponding to standard and new detectors, acquired with no low-cut filtering, 100-Hz low-cut filtering, and 240-Hz low-cut filtering. While the event character and signal amplitudes on the unfiltered records are similar, some differences are evident on the filtered ones. The largest differences are noticed in the 240-Hz low-cut filtered records (the high-frequency components of the airwave and the direct P-wave are more pronounced on the traditional SH-wave seismogram).

The analysis of energy and amplitudes are shown in Figure 13. An interesting result is that, for all filter settings, the energy, the maximum amplitude in the trace, and the maximum reflected amplitude are always higher in the data recorded with the new horizontal detector, even though they were obtained using only half the source energy. This may seem obvious, but it is only apparently so. In fact, the output of the new detector is the sum of its two element outputs, but twice as many blows were necessary to obtain all seismograms recorded with standard geophones. Therefore, energy and amplitude curves quantify the better energy efficiency of the new detectors.

Spectral characteristics are presented in amplitude-versus-frequency plots in Figure 14. Four traces for each record are used for spectra calculations; spectra corresponding to the same number trace are superimposed on each amplitude-versus-frequency plot. It is quite evident that in the 240-Hz low-cut filtered data, mainly for the far-offset traces, the frequency content above 150 Hz is greater in standard geophone data than in new detector data. This fact, already observed in the seismograms in Figure 12 (note the greater amplitudes of the airwave and the direct P-wave), can be read as an index of a better capacity of the new detector to reject P-waves.

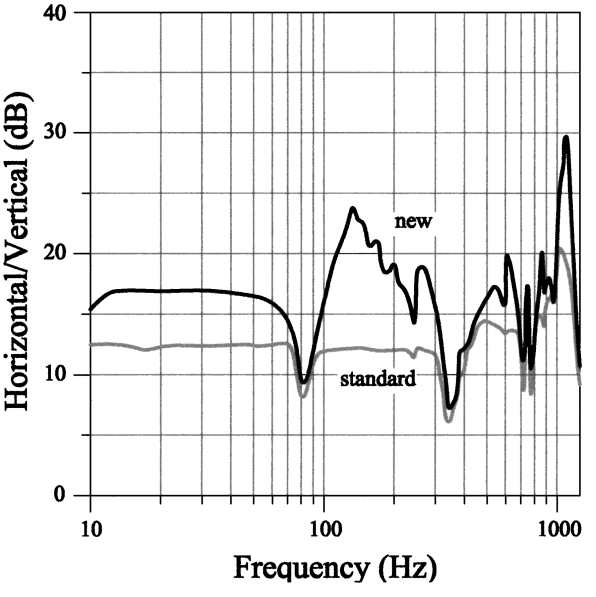

FIG. 8. Amplitude response (horizontal/vertical) ratio for the standard horizontal geophone and the new detector.

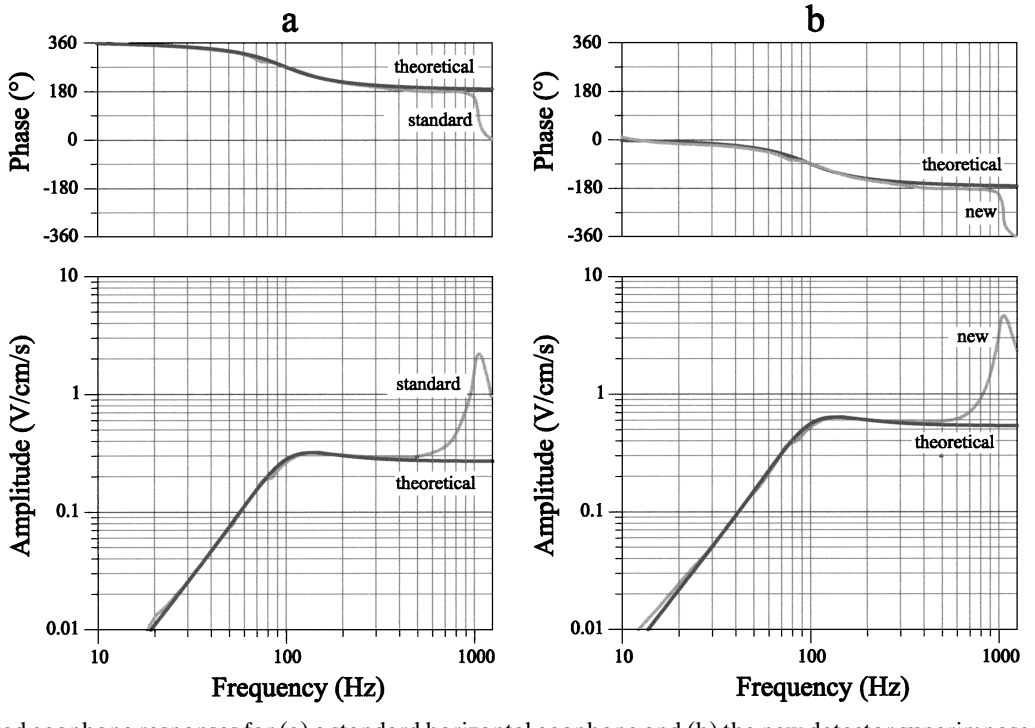

FIG. 7. Calculated geophone responses for (a) a standard horizontal geophone and (b) the new detector superimposed on measured geophone responses.

DISCUSSION

All results prove that the new horizontal velocity detector offers better performance than the standard horizontal geophone. It is, in particular, more highly sensitive to horizontal motion, has higher energy efficiency, and allows cost-effective data acquisition and data processing. In fact, *SH*-wave records can be achieved performing single shots and avoiding the usual *SH*-wave preprocessing, such as time-break variation suppression and amplitude normalization.

The higher sensitivity to horizontal motions derives from two important characteristics: the higher output in the geophone response (Figure 5) and the lower output when excited in the vertical direction (Figure 7). This last aspect needs discussion. We used different low-cut analog filter settings to better highlight the capability of the receivers to enhance *SH*-wave energy and depress *P*-wave energy. It is well known that *P*-waves are richer in high frequencies than *SH*-waves and that low-cut filtering enhances the high spectral content of signals. As expected, as the cut-off frequency increases, the S/N ratio (*SH*-wave amplitude/*P*-wave amplitude) of standard geophone data decreases because the high-frequency components (above all *P*-wave components: airwave and direct *P*-wave) do not cancel efficiently even though time shifting and amplitude rescaling are carefully applied. On the other hand, considering the new detector data, the lower spectral amplitudes above about 150 Hz in the 240-Hz low-cut filtered data are an important index of the capacity of the detector to depress the unwanted *P*-wave components.

The higher sensitivity to horizontal motions and higher energy efficiency of the new type receiver, when mounted together with a vertical geophone, allow vertical- and horizontal-motion data acquisition to be performed simultaneously. Figure 15 shows a vertical- plus horizontal-motion record (interpreted in this case as *P*- plus *SH*-wave record) acquired with a 48-channel ABEM Mark VI seismograph. Odd channels recorded vertical-component (*P*-wave) signals, while even

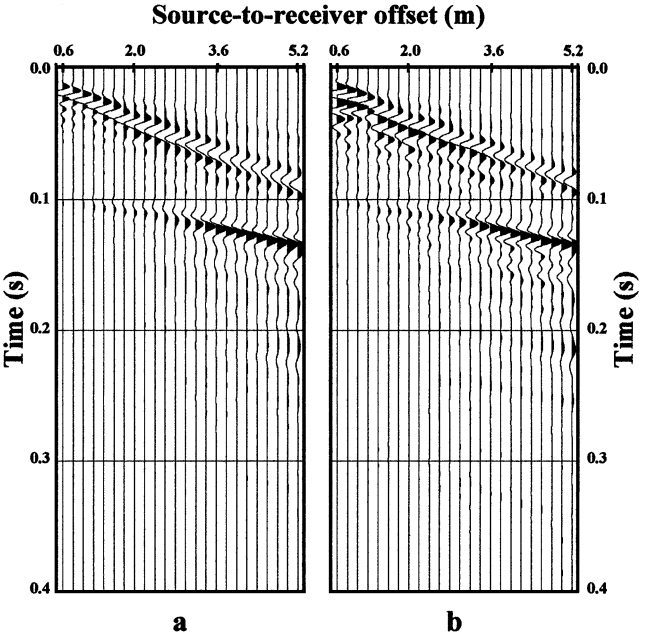

FIG. 10. Raw *SH*-wave seismograms (true relative amplitude) recorded with an analog low-cut filter open. (a) Seismogram obtained with standard geophones using the procedure described in Figure 9. (b) Seismogram obtained with new detectors striking the source in only one direction, that is, using half the source energy.

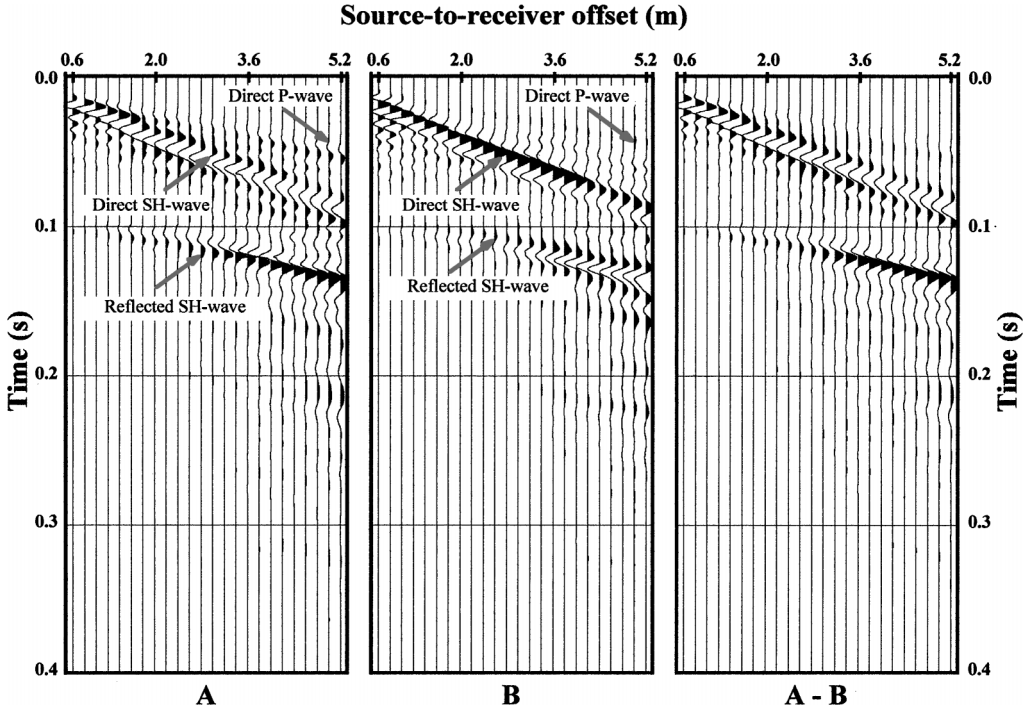

FIG. 9. *SH*-wave summing procedure (A, B) *SH*-wave seismograms recorded striking the source perpendicularly to the receiver line and 180° apart; (A-B) the resulting seismograms of the procedure. Both (A) and (B) were processed for checking and removing time-break variations and for amplitude adjustments (rescaling).

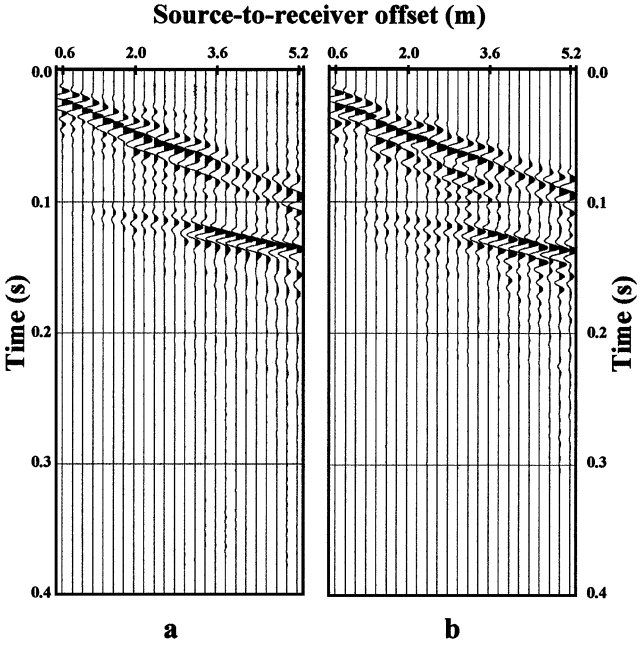

FIG. 11. Raw *SH*-wave seismograms (true relative amplitude) recorded with a 100-Hz analog low-cut filter setting. (a) Seismogram obtained with standard geophones using the procedure described in Figure 9. (b) Seismogram obtained with new detectors striking the source in only one direction, that is, using half the source energy.

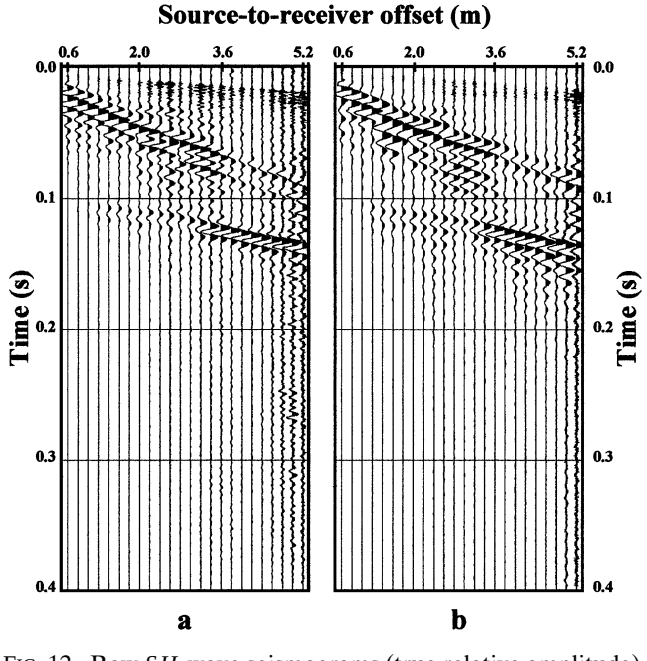

FIG. 12. Raw *SH*-wave seismograms (true relative amplitude) recorded with a 240-Hz analog low-cut filter setting. (a) Seismogram obtained with standard geophones using the procedure described in Figure 9. (b) Seismogram obtained with new detectors striking the source in only one direction, that is, using half the source energy.

channels recorded horizontal-component (*SH*-wave) signals. The vertical- and horizontal-motion records can be obtained by trace sorting.

CONCLUSIONS

We have reported the results of a comparison between a standard horizontal geophone and a newly designed horizontal velocity detector. All tests give sufficient evidence that the new detector, at least for the 100-Hz prototype considered in this study, records horizontal components of a wavefield more faithfully than standard horizontal geophones. Nevertheless, the need for twice as many geophones is certainly a drawback because the new detector is heavier and more costly. We believe, however, that its better technical characteristics and the comparative inexpensiveness of its use outweigh the obvious disadvantage and make it an improvement in *SH*-wave reflection seismology that could be of great assistance to engineering

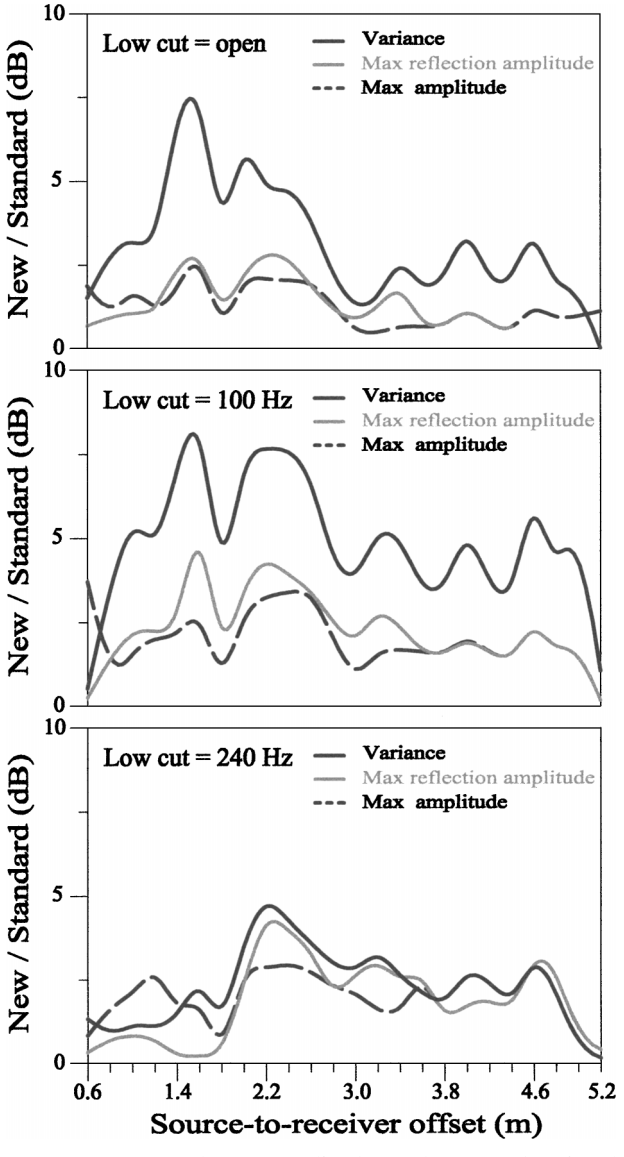

FIG. 13. Energy and true amplitude analyses of the signals recorded with the two types of receivers.

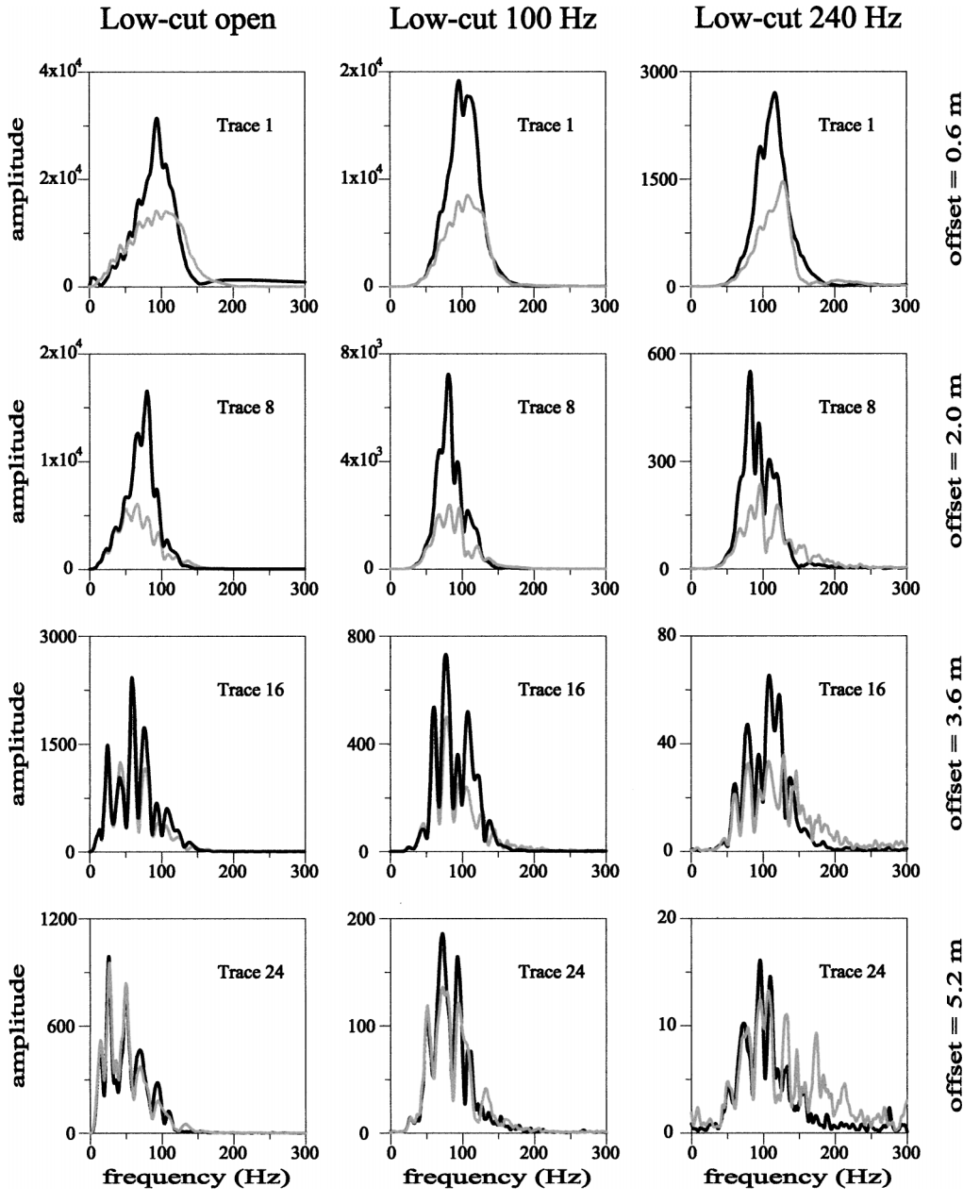

FIG. 14. Amplitude spectra of signals recorded with new detectors (black lines, one shot) and standard geophones (gray line, two shots). In the spectra relative to the 240-Hz low-cut filtered records for frequencies above 150 Hz, the amplitudes in standard geophone data are higher than those in the new detector data.

seismologists. Further tests are being made with receivers of different natural frequency as well as with receivers of other manufacturers.

ACKNOWLEDGMENTS

We are grateful to Valentina Socco for her help in the laboratory tests. We thank Martha Kane Savage, an anonymous reviewer, and Steven L. Roche (Associate Editor) for their careful and constructive reviews that improved the content and clarity of the paper. The efforts of M. A. Melis during manuscript preparation are greatly appreciated. Additional thanks are extended to Luigi Noli, Lai Antonello, Serci Maurizio, Mario Sitzia, and Casti Giampiero for their superlative field work.

REFERENCES

Birkelo, B. A., Steeples, D. W., Miller, R. D., and Sophocleous, M. A., 1987, Seismic-reflection study of a shallow aquifer during a pumping test: Ground Water, **25**, 703–709.

Clark, J. C., Johnson, W. J., and Miller, W. A., 1994, The application of high resolution shear wave seismic reflection surveying to hydrogeological and geotechnical investigations: Symp. on Appl. of Geophys. Eng. and Environ. Problems, Environ. Eng. Geophys. Soc., Proceedings, 231–245.

Dobecki, T. L., 1993, High resolution in saturated sediments—A case for shear wave reflection: Symp. on Appl. of Geophys. to Eng. and

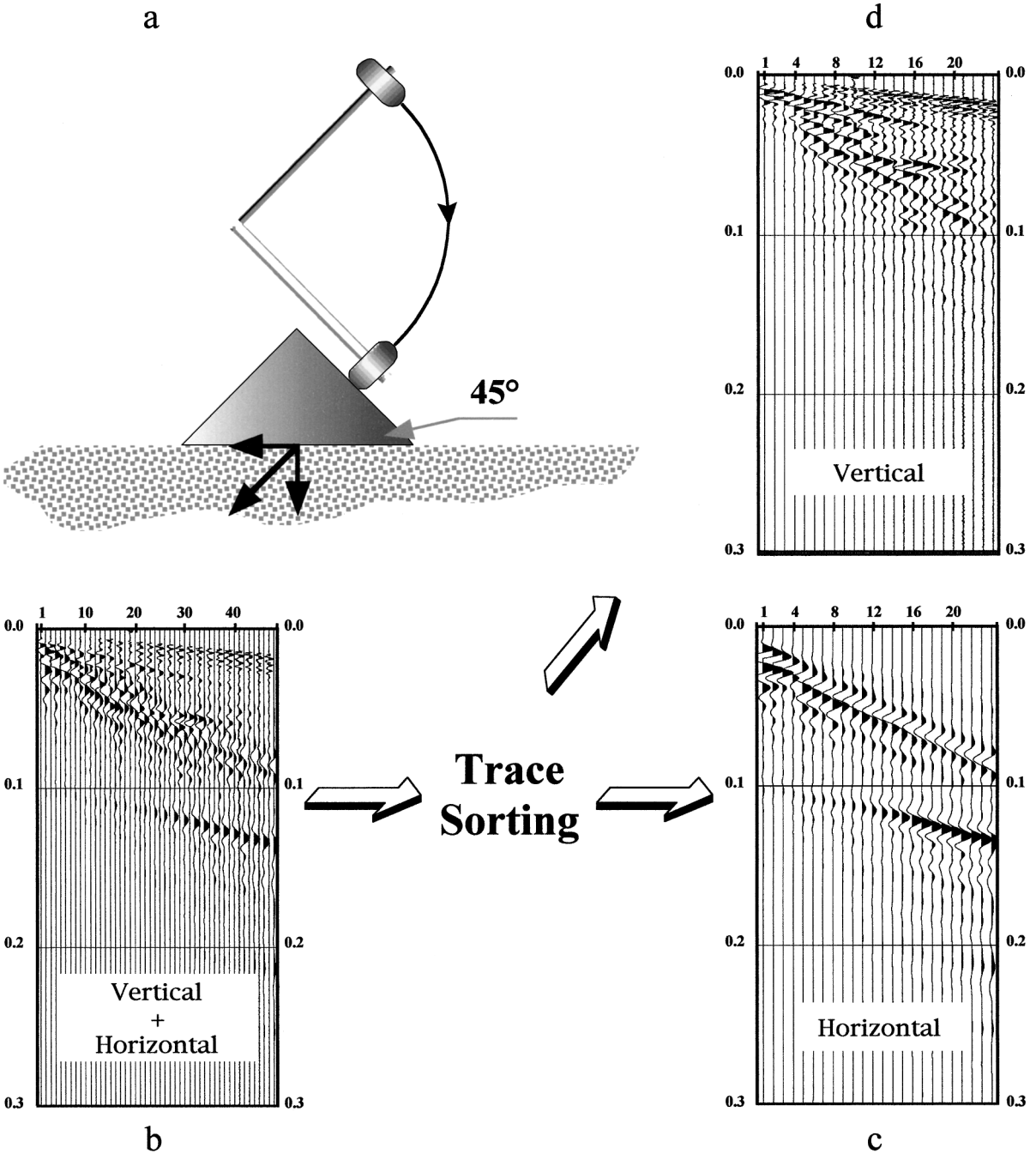

FIG. 15. Example of simultaneous vertical- and horizontal-motion data acquisition. (a) Schematic of the source used for generating simultaneous vertical and horizontal motion. The sledgehammer strikes the prismatic baseplate at an angle 45° from the vertical, swinging on a plane perpendicular to the source–receiver direction. (b) Vertical- plus horizontal-motion seismogram, interpreted in this case as a *P*- plus *SH*-wave seismogram. (c) Even traces in (b); this seismogram coincides with that shown in Figure 10b. (d) Odd traces in (b); the following coherent events are evident on this seismogram: the high-frequency airwave, the direct *P*-wave, the reflected *P*-wave, and surface (Rayleigh) waves.

Environ. Problems, Environ. Eng. Geophys. Soc., Proceedings 319–333.
Doornenbal, J. C., and Helbig, K., 1983, High-resolution reflection seismics on a tidal flat in the Dutch Delta—Acquisition, processing and interpretation: First Break, **1**, No. 5, 9–20.
Goforth, T., and Hayward, C., 1992, Seismic reflection investigations of a bedrock surface buried under alluvium: Geophysics, **57**, 1217–1227.
Hasbrouck, W. P., 1991, Four shallow-depth, shear-wave feasibility studies: Geophysics, **56**, 1875–1885.
Helbig, K., 1987, Shear-waves—What they are and how they can be used, *in* Danbom, S. H., and Domenico, S. N., Eds., Shear-wave exploration: Soc. Expl. Geophys., Geophysical Development Series **1**, 19–36.
Hunter, J. A., Pullan, S. E., Burns, R. A., Gagne, R. M., and Good, R. L., 1984, Shallow seismic reflection mapping of the overburden-bedrock interface with the engineering seismograph—Some simple techniques: Geophysics, **49**, 1381–1385.
Jeng, Y., 1995, Shallow seismic investigation of a site with poor reflection quality: Geophysics, **60**, 1715–1726.
Jongerius, P., and Helbig, K., 1988, Onshore high-resolution seismic profiling applied to sedimentology: Geophysics, **53**, 1276–1283.

McCormack, M.D., and Tatham, R. H., 1986, Shear-wave exploration seismology: Soc. Expl. Geophys., Continuing Education Program, Course Notes.
Milkereit, B., Stumpel, H., and Rabbel, M., 1986, Shear wave reflection profiling for near-surface lignite exploration: Geophys. Prosp., **34**, 845–855.
Miller, R. D., and Steeples, D. W., 1990, A shallow seismic reflection survey in basalts of the Snake River plain, Idaho: Geophysics, **55**, 761–768.
———1991, Detecting voids in a 0.6-m coal seam, 7 m deep, using seismic reflection: Geoexploration **28**, 109–119.
Miller, R. D., Steeples, D. W., and Brannan, M., 1989, Mapping a bedrock surface under dry alluvium with shallow seismic reflections: Geophysics, **54**, 1528–1534.
Sambuelli, L., and Deidda, G. P., 1998, Trasduttore di onde elastiche con sensibilità incrementata alle onde di taglio: Italian Patent TO98A000030.
———1999, "Swyphone": A new seismic sensor with increased response to *SH*-waves: Presented at the 5th Mtg., Environ. Engin. Geophys. Soc. Europ. Sect.
Singh, S., 1986, Reflection-window mapping of shallow bedrock: Geophys. Prosp., **34**, 492–507.
Steeples, D. W., and Miller, R. D., 1990, Seismic reflection methods applied to engineering, environmental, and groundwater problems, *in* Ward, S., Ed., Geotechnical and environmental geophysics, **I**: Review and tutorial: Soc. Expl. Geophys., 1–30.
Steeples, D. W., Green, A. G., McEvilly, T. V., Miller, R. D., Doll, W. E., and Rector, J. W., 1997, A workshop examination of shallow seismic reflection surveying: The Leading Edge, **16**, 1641–1647.
Stumpel, H., Kahler, S., Meissner, R., and Milkereit, B., 1984, The use of seismic shear waves and compressional waves for lithological problems of shallow sediments: Geophys. Prosp., **32**, 662–675.
Ziolkowski, A., and Lerwill, W. E., 1979, A simple approach to high resolution seismic profiling for coal: Geophys. Prosp., **27**, 360–393.